Effect of rippled field on energetic ion confinement in 15MA scenario in ITER

K. Shinohara, K.Tani, S. Putvinski
Japan Atomic Energy Agency, Naka, Ibaraki 311-0193, Japan
Nippon Advanced Technology Co., Ltd., Naka Office, Naka, Ibaraki, Japan
ITER Organization, Route de Vinon sur Verdon, F-13115 St Paul lez Durance, France
shinohara.koji@jaea.go.jp

1. Introduction

It is well known that the non-axisymmetric field, called as the rippled field here, can induce the enhanced transport of the energetic ions. In the ITER design, the allowable heat load induced by the energetic ions is still marginal and should be less than 0.1 MW/m2 except for the divertor region because the dominant heat load from the bulk plasma is large. The energetic ion confinement is also required to be the level similar to that in the axisymmetric field because the plasma heating and the current drive are based on the energetic ion confinement in the axisymmetric field. There are several sources of the rippled field, such as the discreteness of toroidal field coils (TFC), the ferromagnetic material, and the ELM mitigation/control coil, referred as ELMC below. The design of the installation of the ferromagnetic material, and ELMC is on going as well as the design of a wall shape and operation scenarios. Reflecting this situation, the assessment of the energetic ion losses due to the rippled field using the latest design is still an important subject in the ITER design. In addition to the assessment that has been carried out for the effect of the ferromagnetic material since 2007[1], we have started the assessment of the effect of the ELMC recently by using the F3D OFMC code, which is a guiding-center-orbit following Monte-Carlo code[2],[3]. It was found that the NB ion, which was produced by NBI, confinement could be reduced in the operation Scenario 4 when ELMC was energized [4].

We carried out the F3D OFMC calculation to evaluate the energetic ion confinement in the environment based on the recent information about the equilibrium for 15 MA Scenario, the first wall geometry, the implementation of ferritic inserts (FI), and the ELMC. Here, 15MA Scenario means the operation scenario, which has been developed recently, for an inductive scenario with a full bore plasma producing 500 MW of fusion power with Q=10 for 400s. Note that the scenario is similar to but somewhat different from the one called Scenario 2 [5].

2. Calculation condition

First wall shape

As mentioned in Ref [6], the wall shape can change not only the heat load distribution but also the characteristics of the escaping ions, such as their energy distribution. Considering the contribution to the actual ITER design, we used the most recent wall shape design, which is distributed by the ITER organization (IO). The 3D wall shape is shown in Fig. 1. From the requirement to reduce the wall load due to the bulk plasma, a corrugated first wall shape is proposed. The structure has a 36-fold toroidal symmetry. The port opening and other structures are not considered in this calculation.

Equilibrium and profiles of plasma parameters

The study of the plasma operation scenario is on going in the fusion community under the IO. At present, there are varieties of "15MA scenario". In this study, I used the 15MA scenario, which is used for the design studies of the ELM coil, based on the transport study of the bulk plasma by CORSICA code[8],[9]. The equilibrium and wall shape at the toroidal angle of 1.53 degree, where the wall is closest to the plasma, is plotted in Fig. 2(a).

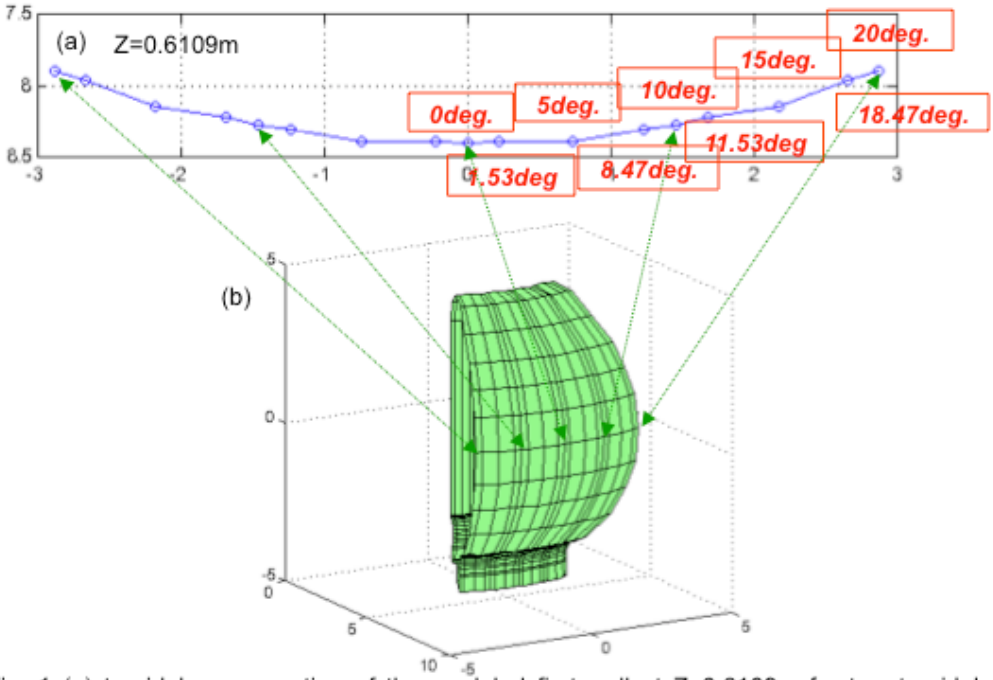

Fig. 1 (a) toroidal cross section of the modeled first wall at Z=0.6109m for two toroidal sections from -20 to 20 degrees. (b) bird's eye view of the first wall for two toroidal sections

Profiles of n_e, T_e, T_i, and q in this calculation are plotted in Fig. 2(b)-(d). The Z_{eff} is handled as a constant value of 1.71, where the line averaged value is used. Beryllium is employed as an impurity species.

Birth distribution of fast ions

The confinements of two kinds of fast ion species have been assessed. One is a fusion born alpha particle with the energy of 3.5MeV and the other is deuteron produced by two neutral beam injectors, NBIs, with the energy of 1MeV and the power of 33MW in total.

The birth distribution of alpha particles has been calculated from the above mentioned plasma parameters. The birth distribution of fast deuterons due to two NBIs has been calculated, using the geometry of NBIs. The geometry information is described in Ref. [7]. NBIs have the most on-axis alignment with the tangency radius of 5.3 m.

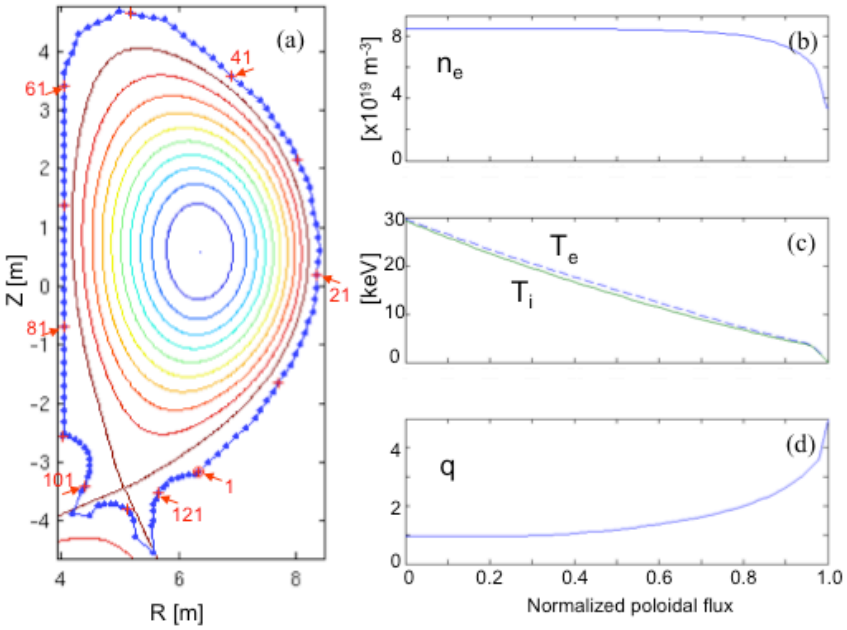

Fig. 2 (a)Equilibrium and wall shape at the toroidal angle of 1.53 degree. The wall node number is labelled beside the wall shape. Profiles for ne(b), Te and Ti(c), and q (d)

Magnetic field

In this paper, the fast ion confinement is

evaluated for the background by the TFC alone, TFC+FI, and TFC+FI+ELMC. The magnitude of the TF at R=6.2m and Z=0.0 m is 5.3T. The magnetic background by TFC+FI is supplied by the IO; the magnetic background is calculated by St. Petersburg company, not considering the influence of the poloidal field such as plasma current on FI, but considering the irregular sectors around the NB ports between 50º and 100º. Fig. 3 shows the magnetic field variation by the TFC+FI. The magnetic background by TFC alone and ELMC alone is calculated, based on the coil design distributed by the IO. The background magnetic field for the case by TFC+FI+ELMC is produced by adding the vacuum field generated by the ELMC to that by TFC+FI. Namely, the shielding effect of the field penetration by plasma is not considered in this analysis.

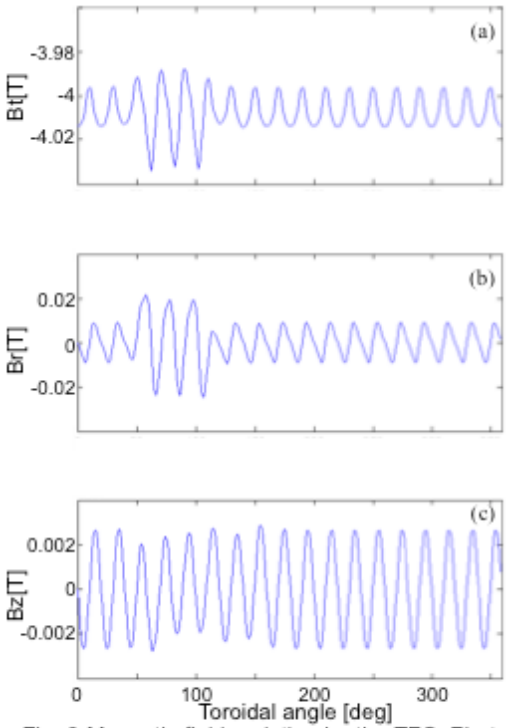

Fig. 3 Magnetic field variation by the TFC+FI at the position of (R,Z)=(8.2m, 0.6m). (a)Bt,(b)Br, (c)Bz

Because the ELM mitigation field distorts the plasma impact pattern on the divertor targets, the ELM mitigation field pattern will probably be rotated slowly in the toroidal direction, to time-average the thermal load over the divertor targets. However, the rotation is not taken into account in this analysis. This report describes a steady state analysis.

The information about the geometry and the coil currents of ELMC was provided by the IO. Fig. 4 shows the ELMC model. The ELMC is modeled as filament loops. There is one group of 3 ELM coils (upper, middle, and lower rows) on each of the 9 vessel sectors which are centered on the toroidal angles, $\phi_{i=\{1,2,..,9\}}$, of 30º, 70º, 110º, ..., 350º. Here, the toroidal angle starts from the middle of the TFC-1 and increases in the counter-clock-wise direction. The field of ELMC was calculated by the coil current described as $I_{ij} = I_{coil} \cos [n (\Delta\phi_j - \phi_i)]$, where I_{coil} is the maximum value of the current in the coils, n is the toroidal mode number, ϕ_i is the toroidal angle of the toroidal sector as mentioned above, and $\Delta\phi_{j=\{top,middle,bottom\}}$ is the phase shift. The coil current information provided by the IO was derived from the calculation based on experiments at DIII-D [10]- [13]. We have assessed the fast ion confinement for the following three field fields;

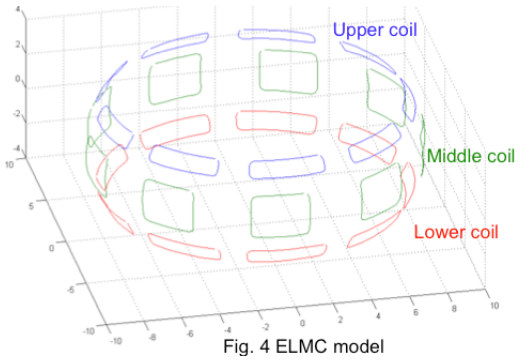

Fig. 4 ELMC model

1. Min_n4 field: I_{coil} = 30 kAt with $\Delta\phi_{top} = 52^o$, $\Delta\phi_{middle} = 0^o$, is $\Delta\phi_{bottom} = 38^o$. This is the minimum I_{coil} to achieve the required level of edge magnetic field perturbation for the n=4 cosine waveform. Here we refer to this case as Min_n4 field.
2. Min_n3 field: I_{coil} = 45 kAt with $\Delta\phi_{top} = 86^o$, $\Delta\phi_{middle} = 0^o$, is $\Delta\phi_{bottom} = 34^o$. This is the minimum I_{coil} to achieve the required level of edge magnetic field perturbation for the n=3 cosine waveform. Here we refer to this case as Min_n3 field.

3. Max_n4 field: I_{coil} = 90 kAt with $\Delta\phi_{top} = 36^o$, $\Delta\phi_{middle} = 0^o$, is $\Delta\phi_{bottom} = 50^o$. This provides the maximum level of edge magnetic field perturbation for the n=4 cosine waveform. Here we refer to this case as Max_n4 field.

The vacuum magnetic field produced solely by the ELMC is plotted in Fig. 5 for the Min_n4, Min_n3, and Max_n4 fields.

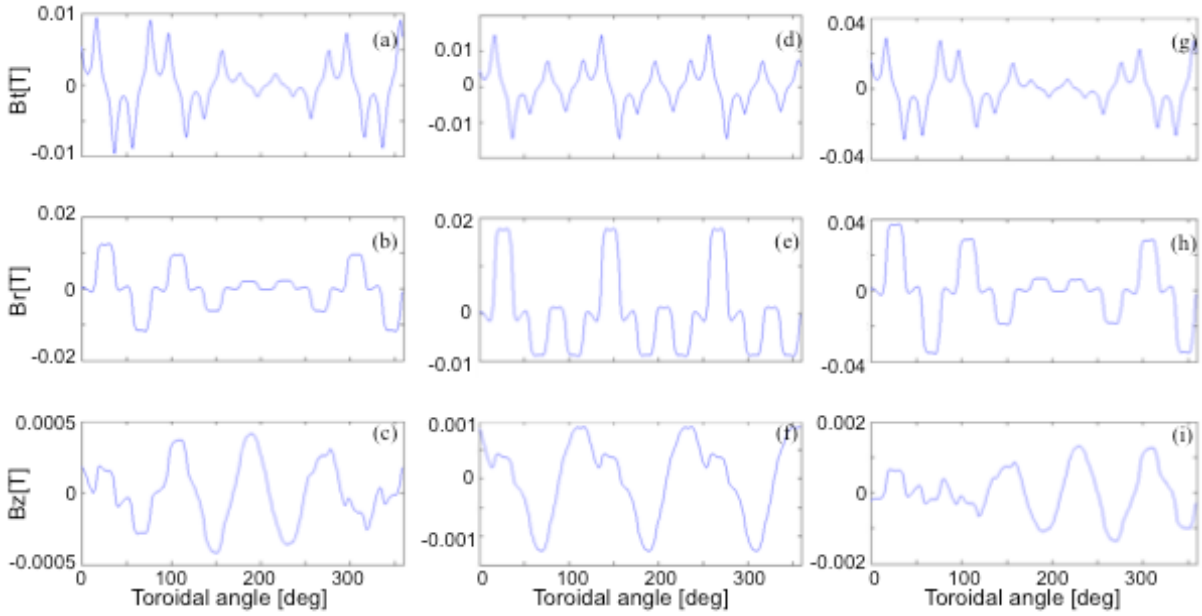

Fig. 5 Magnetic field variation produced solely by the ELMC at the position of (R,Z)=(8.2m, 0.6m). (a-c) for the Min_n4 pattern, (d-f) for the Min_n3 pattern, (g-i) for the Max_n4.

3. Calculation results

The calculations were carried out, changing the magnetic field and the fast ion species. The simulation condition and its result are summarized in **Table 1**.

Table 1

ID	Fast ion species	Magnetic field	Loss power fraction [%]	Maximum heat load [MW/m^2]	Contribution of >2.8 MeV for alpha and >0.8 MeV for NB ions in loss power [%]	Number of test particles
1-alpha	alpha	Case1: TFC alone	0.8	0.06	47.8	27,000
1-NB	By NB	Case1: TFC alone	0.8	0.02	0	13,600
2-alpha	alpha	Case2: TFC + FI	0.04	<0.01	68.3	27,000
2-NB	By NB	Case2: TFC + FI	0.05	<0.01	0	13,600
3-alpha	alpha	Case3: TFC + FI + Min_n4	0.95	0.06	56.5	27,000
3-NB	By NB	Case3: TFC + FI + Min_n4	7.5	0.27	54.9	13,600
4-alpha	alpha	Case4: TFC + FI + Min_n3	1.6	0.06	53.8	27,000
4-NB	By NB	Case4: TFC + FI + Min_n3	10.0	0.21	38.3	13,600

5-alpha	alpha	Case5: TFC + FI + Max_n4	6.2	0.21	65.9	27,000
5-NB	By NB	Case5: TFC + FI + Max_n4	26.2	0.36	67.7	13,600
6-alpha	alpha	Case6: Axisymmetric TF + Min_n4	0.9	0.06	56.6	27,000
6-NB	By NB	Case6: Axisymmetric TF + Min_n4	7.0	0.24	56.7	13,600
7-NB	By NB	Case7: Axisymmetric TF + (n=4, 30kAt, zero phase difference between upper, middle, lower coils)	0.6	0.03	20.9	13,600
8-NB	By NB	Case8: Axisymmetric TF + (n=4, 15kAt)	2.4	0.09	32.4	13,600

When we compare the cases 1 and 2, we can see the effectiveness of the FI in the fast ion confinement. The loss power fraction is reduced to the level of less than 0.1% for both alpha particles and NB ions. The contribution of the alpha particles with the energy of >2.8 MeV is around 50% in the loss power. That of the NB ions with > 0.8MeV is about 0%, namely the loss ions are mostly slow-down ions. It is considered that the NB ions are well confined because the NB ions are injected tangentially in the same, CO-, direction to the plasma current.

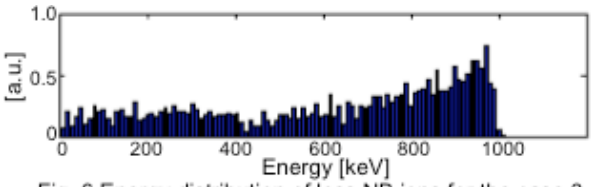

Fig. 6 Energy distribution of loss NB ions for the case 3

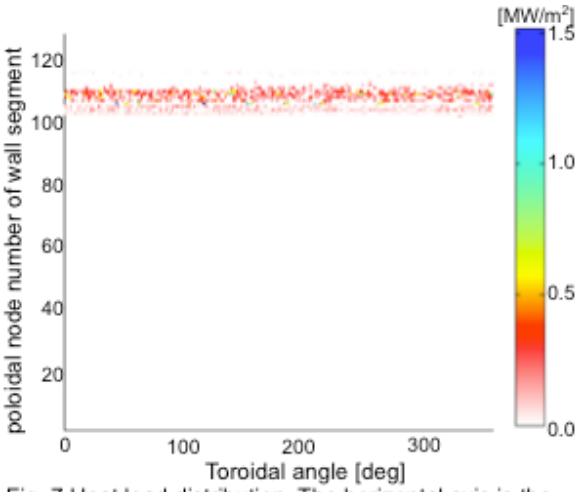

Fig. 7 Heat load distribution. The horizontal axis is the toroidal angle. The vertical axis is the poloidal node number of the wall segments, which is labeled in Fig. 2

The results with the ELMC field in addition to the field by the TFC and the FI correspond to the cases 3 – 5. The loss power fraction is increased to the level above that for TFC alone. The effect of the ELMC field is especially larger for NB ions. The contribution of the NB ions with the energy of >0.8 MeV increases to larger than 50%. The energy distribution of loss NB ions for the case 3 (Min_n4 field) is plotted in Fig. 6 as an example. This suggests a part of NB ions are lost before the slow-down without transferring their energy to the bulk plasma.

For the comparison, we carried out the calculation under the magnetic field in which the vacuum ELMC field for the case of Min_n4 were added to the axisymmetric TF in a tokamak system. Here, the axisymmetric TF is defined by the formula Bt_{axis} x R_{axis} /R=32.86/(R[m]) [T]. The results for the case 6 are similar to those for the case 3. This indicates that the loss of fast ions is determined by the ELMC field.

The heat load is observed in the most cases in the divertor region. As an example, the heat load by NB ions for the case 3 is shown in Fig. 7. The

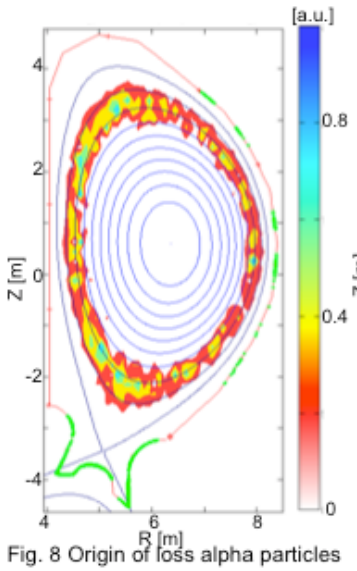

Fig. 8 Origin of loss alpha particles

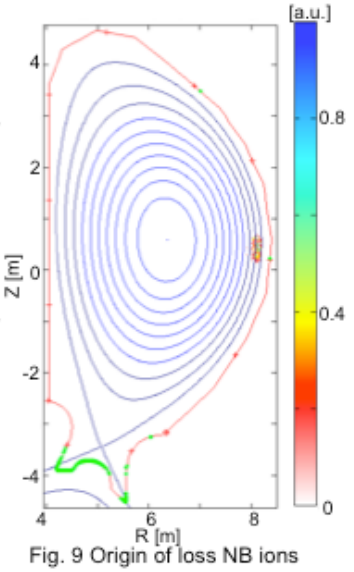

Fig. 9 Origin of loss NB ions

divertor region corresponds to the node number 95-120 of the wall segments. Here, the charge exchange between neutral gas and fast ions is not considered in this calculation. The charge exchange can broaden the area of the heat load though the cross section of the charge exchange is small for fast ions. The error of the heat load comes from the number of test particles, which hit a wall segment. The error is relatively large in this divertor region because of the fine shape, namely the small surface area of a wall segment in this region. The difference of the space structure of the magnetic field can change the heat load footprint, however we need much larger number of test particles to investigate the difference of the footprint. This investigation is out of the scope in this work. Here, we averaged the heat load in the toroidal direction, considering the following conditions; 1) the ELM mitigation field will be rotated slowly in the toroidal direction as mentioned above, 2) the wall shape is axisymmetric in this region, and 3) the ripple field except for the ELMC is small in this region. Assuming the field will rotate continuously, we averaged the heat load over 18 sectors in the toroidal direction. The maximum heat load in **Table 1** is a result of this averaging. The heat load due to the alpha particles plus NB ions can be an allowable level though it depends on the level of the heat load by the bulk plasma.

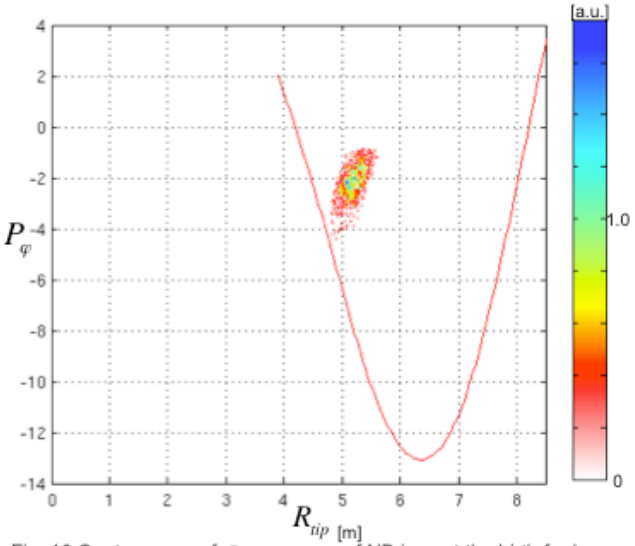

Fig. 10 Contour map of P_φ versus R_{tip} of NB ions at the birth for loss NB ions for the case 3

The distribution of the origin of the loss alpha particles is depicted for the case 3 in Fig. 8. The alpha particles born in the region where the normalized poloidal flux is larger than 0.7 are expelled. It is considered that this distribution is determined both by the region of the magnetic perturbation and by the initial birth profile of alpha particles, which are produced by d-T reaction.

The distribution of the origin of the loss NB ions is also depicted for the case 3 in Fig. 9. The NB ions generated in the region where the normalized poloidal flux is larger than 0.85 are mainly expelled in this case. To understand the characteristics of the loss NB ions, we

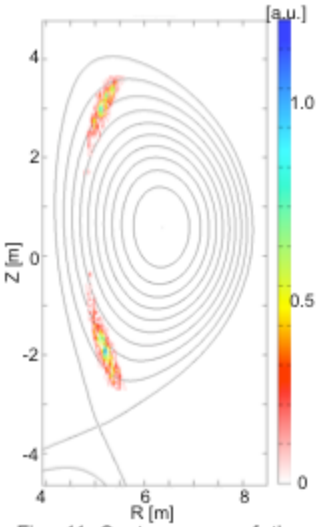

Fig. 11 Contour map of the banana tip of NB ions at the birth for loss NB ions

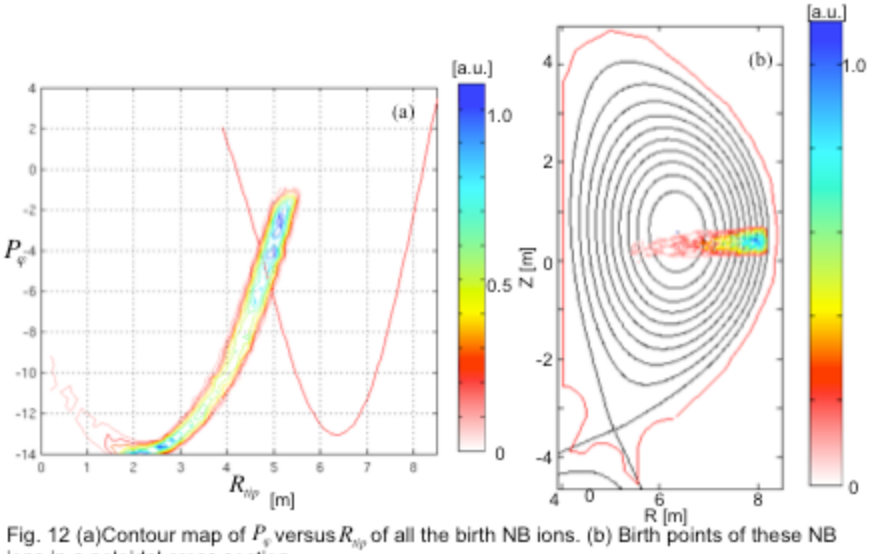

Fig. 12 (a)Contour map of P_φ versus R_{tip} of all the birth NB ions. (b) Birth points of these NB ions in a poloidal cross section.

plotted the contour map of P_φ versus R_{tip} of the loss NB ions at the birth as well as the curve of the poloidal flux in Fig. 10. Here, P_φ is a canonical toroidal angular momentum defined by the formula, $P_\varphi = \psi_{fast} - \frac{m_{fast}}{q_{fast}} R_{fast} v_\varphi$, and R_{tip} is defined by the formula, $R_{tip} = \left(\frac{v_\perp}{v}\right)^2 R_{fast}$. When the value of ($R_{tip}$, P_φ) lies above the curve of the poloidal flux and below zero in this figure, the corresponding particle is trapped in the axisymmetric tokamak. Interestingly, Most of the loss NB ions are trapped at the birth. Fig. 11 shows the contour map of the banana tip position of the above-mentioned trapped ions for the loss NB ions. The banana tips of the most ions exist in the region where the normalized flux is larger than 0.7. Then, Fig. 12(a) shows the contour map of P_φ versus R_{tip} for all of the NB ions at the birth, and Fig. 12(b) shows the contour map of the birth points for these ions in a poloidal section. It is found that many NB ions are generated as trapped particles, even though the NB is injected in a shallow tangential angle. The reason exists in the fact that many NB ions are generated in the peripheral region as seen in Fig. 12(b) because of the high temperature and high density of the target plasma. The pitch angle of the NB ion becomes larger due to a geometrical reason when the NB ion is generated at the peripheral region for a NB injector. These trapped NB ions with a large population dominantly contribute to the large loss by the ELMC field. Thus, the further penetration might reduce the ratio of the trapped NB ions. Therefore, one option could be to change the plasma shape to reduce the most outer plasma position. Another option could be to use higher energy NB, though these options are not so easy.

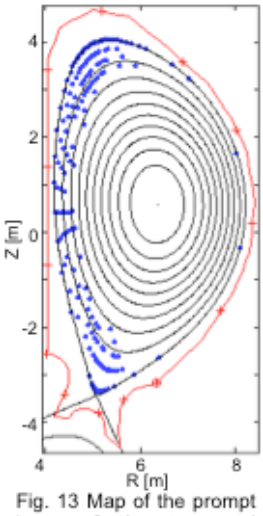

Fig. 13 Map of the prompt loss of the trapped deuterons with the energy of 1MeV for the case 6

In the case of the Min_n4 field, the phase difference between the middle and upper coils, and the middle and lower coils are optimized, considering the effective edge magnetic field perturbation. We investigated the effect of the phasing of the ELMCs in the case 7. The phase difference is set to zero, keeping the coil current same with that for the Min_n4 field. The loss power fraction is reduced to the level in the case of the TFC alone. It is considered the optimized magnetic field perturbation is effective in the deterioration of the fast ion confinement.

We reduced the coil current to the half of the case of the Min_n4 field in order to investigate the dependence of the coil current magnitude on the loss fraction in the case 8, keeping the phase difference. It is found that the loss fraction of NB ions is reduced to one-third of the case of the Min_n4 field and that the dependence is stronger than the linear one. This result also indicates that the optimized magnetic field perturbation is effective in the deterioration of the fast ion confinement.

A map of the prompt loss region of the trapped ions for the case of the Min_n4 field (the case 6) has been made. In making this map, at first, 1 MeV NB ions with the pitch, $v_{//}$ / v, of zero were distributed as the birth distribution uniformly on the coordinate of the poloidal angle and the psi. This means all the birth particles start to move from the banana tip of their orbit. Next, the particles were traced for 20 ms, considering collision process. Then, we plot birth points of the particles lost in this short time period. Fig. 13 shows the result. The region is close to the area of the banana tip at the birth for the loss NB ions (Fig. 11).

We have traced the guiding center orbits for 1 MeV NB ions with the pitch, $v_{//}$ / v, of one, namely for pure co-passing ions, without collisions. The start positions of the ions are at the toroidal angle of zero and at the poloidal angle of zero. The canonical toroidal angular momentum was written down at every time when the NB ions passed through the toroidal angle of zero. The variation of the canonical toroidal angular momentum becomes large in the

peripheral region. This result suggests that the co-passing fast ions can be affected by this magnetic perturbation in this region, and the diffusion can be increased under the circumstance with a collision.

The 3.5MeV alpha particles and the 4.5keV deuterons generated on the surface of the normalized flux of 0.91, which corresponds to the pedestal position, were traced for the axisymmetric TF field alone and the axisymmetric TF plus Min_n4 field (the case6) with taking into account the collision. The birth position is illustrated in Fig. 14. The pitch angle distribution of the particles is uniform in the velocity space. The calculation results are plotted as the temporal evolution of accumulated loss particle fraction in Fig. 15. The results indicate the confinement deteriorates and the loss relatively in a short time scale increases even for low energy particles as well as high energy particles.

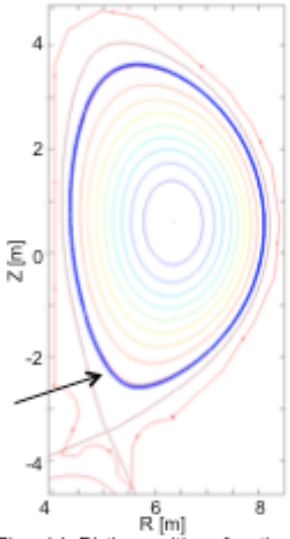

Fig. 14 Birth position for the particles generated at the surface of the normalized flux of 0.91. The pitch angle distribution of the particles is

4. Summary

In this paper, we reported the results of the F3D OFMC calculation for the fast ion confinement based on the most recent information about the equilibrium for 15 MA Scenario, the first wall geometry, the implementation of ferritic inserts (FI), and the ELMC.

The alpha particles and 1MeV NB ions are well confined and the heat load on the first wall is negligible and allowable for the magnetic background by the TFC and FI. However, some deterioration of the confinement of these fast ions is observed when the magnetic field by the optimized ELMC field is applied as the vacuum field. The similar level of the deterioration is observed under the magnetic filed solely by the optimized ELMC field.

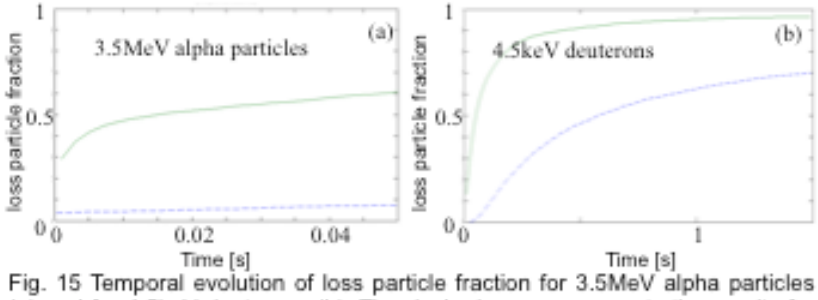

Fig. 15 Temporal evolution of loss particle fraction for 3.5MeV alpha particles (a) and for 4.5keV deuterons (b). The dashed curve represents the results for the axisymmetric TF field alone and the solid curve represents the results for the axisymmetric TF plus Min_n4 field (the case6)

The induced loss is larger for the NB ions than for alpha particles under the ELMC field. For NB ions, the origin of the loss ions is dominantly trapped ions generated in the peripheral region due to the high temperature and high density plasma of 15 MA Scenario.

The origin of the loss fast ions is peripheral region. We need to evaluate the local effect of the loss on the peripheral plasma. The evaluation needs much more test particles and is considered to be a future work.

In this study, the shielding effect of plasmas on field penetration is not considered because an appropriate model of the shielding effect is still missing. The results can be changed under the magnetic background where the shielding effect of plasmas is taken into account. We are planning to reevaluate the fast ion confinement when the appropriate magnetic background is available.

The views and opinions expressed herein do not necessarily reflect those of the ITER Organization

Acknowledgments

We would like to thank to Drs T. Oikawa, A. Loarte, M. Schaffer, T. Casper, T. Evans

for their providing us the information for the calculation. On of authors, K. Tani, would like to express appreciation to Drs Y. Kusama and T. Sugie for their support of this work.

Reference

[1] Shinohara K., *et al*, Fusion Engineering and Design 84 (2009) 24

[2] Tani K., *et al*, J. Phys. Soc. Jpn., 50 (1981) 1726

[3] Shinohara K., *et al*, Nucl. Fusion 43 (2003) 586

[4] Tani K., *et al* , submitted to Nucl. Fusion

[5] Polevoi A.R., Medvedev S.Yu., Mukhovatov V.M., *et al*, J. Plasma Fusion Res. SERIES, Vol. 5 (2002) 82–87

[6] Shinohara K., *et al*, Nucl. Fusion 51 (2011) 063028

[7] ITER Technical Basis, Chapter 2.5, G A0 FDR 1 01-07-13 R1.0 , Private Communication.

[8] Crotinger J.A. et al 1997 LLNL Report UCRL-ID-126284, available from NTIS #PB2005-102154 ,

[9] Casper T.A. *et al* Nucl. Fusion 51(2011) 013001

[10] Evans T.E., Fenstermacher M.E., Moyer R.A. et al 2008 Nucl. Fusion 48 024002

[11] Fenstermacher M.E., Evans T.E. Osbone T.H. et al 2008 Physics of Plasmas 15 056122

[12] Schaffer M.J. et al 2008 Nucl. Fusion 48 024004

[13] Orlov D.M., et al, "Analysis of edge magnetic field line structure in ITER due to in-vessel ELM control coils", General Atomics Report GA–A27049, submitted to Fusion Engineering and Design